

Real Time Simulation of Grasping Procedure of Large Internal Organs during Laparoscopic Surgery

Hossein Dehghani Ashkezari, Alireza Mirbagheri, Farzam Farahmand, Saeed Behzadipour,
Keikhosrow Firoozbakhsh

Abstract— Surgical simulation systems facilitate safe and efficient training processes of surgical trainees by providing a virtual environment in which the surgical procedure can be repeated unlimitedly in a wide variety of situations. The present study attempted to develop a real time simulation system for the grasping procedure of large internal organs during laparoscopic surgery. A mass-spring-damper model was developed to simulate the nonlinear viscoelastic large deformations of the spleen tissue while interacting with a triple-jaw grasper. A novel collision detection algorithm was designed and implemented to determine the contact points between the tissue and the grasper jaws. Force or geometrical based boundary conditions were imposed at the contact nodes, depending upon the relative magnitudes of the external pull force and the tangential component of the contact force. The efficacy of the model to calculate and render the grasper-spleen interactions in real time was examined in a number of simulations. The results of the model were qualitatively acceptable. The deformation of the tissue was realistic and its stress relaxation behavior could be reproduced. Also, the tool-tissue interactions in slippage-free and slippage-accompanied grasping conditions could be replicated when appropriate coefficients of friction were employed.

I. INTRODUCTION

Laparoscopic surgery is performed in abdominal cavity using long and narrow instruments, which pass through small incisions. [1]. This technique minimizes the patients' trauma and permits a faster recovery in comparison with traditional open surgery [2, 3]. However, with the loss of direct visual and tactile information, it requires a complicated training procedure for the surgeons to obtain sufficient proficiency [4]. The trainees need to practice the hand and eye coordination and learn how to work with instruments with limited maneuverability under fulcrum effect, i.e., moving in the opposite direction of the hand's motion [5]. Surgical simulation systems facilitate safe and efficient training processes by providing a virtual environment in which the

H. Dehghani Ashkezari and A. Mirbagheri are with the Mechanical Engineering Department, Sharif University of Technology, Tehran, Iran and also the Robotic Surgery lab., Research Center of Biomedical Technology and Robotics (RCBTR), Tehran University of Medical Sciences, Tehran, Iran (e-mail: hdehghani@mech.sharif.edu; mirbagheri@mech.sharif.edu).

F. Farahmand is a professor and head of Biomechanics Section at Sharif University of Technology and also head of Robotic Surgery Lab at Research Center of Biomedical Technology and Robotics (RCBTR), Tehran University of Medical Sciences, Tehran, Iran (e-mail: farahmand@sharif.edu).

S. Behzadipour and K. Firoozbakhsh are with the Mechanical Engineering Department, Sharif University of Technology, Tehran, Iran (e-mail: behzadipour@sharif.edu; keikhosrow@gmail.com).

trainee can repeat the surgical procedure unlimitedly at a wide variety of situations [6]. An essential requirement of such systems, however, is functioning in real time. The system shall be able to simulate the tool-tissue interactions with an update rate of at least 30 Hz for graphical rendering [7] and about 1 KHz for driving the haptic device [8].

Real time simulation of the tool-tissue interactions with sufficient accuracy is a difficult task. Biological soft tissues often exhibit complicated mechanical behaviors, including rate dependency [9] and nonlinearity, either due to their inherent material properties [10, 11] or as a result of being largely deformed [12]. On the other hand, the modalities of tool-tissue interactions during surgery are quite diverse and a wide variety of surgical tasks, e.g., indentation [12], cutting [13, 14], and grasping [13] are needed to be simulated. As a result, it is much challenging to integrate an appropriate mechanical model of the tissue with the complicated and diverse tool-tissue interactions happening in surgery [15].

The purpose of the present study was to simulate the interactions of a soft tissue and a surgical tool in a difficult surgical maneuver, i.e., grasping of large soft organs. The simulation was intended to provide acceptable qualitative results, by compensation between the biomechanical realism and real-time computation requirements. The mechanical behavior of the large organ was modeled in detail, including its nonlinear viscoelastic properties. Appropriate boundary conditions were imposed and different coefficients of friction were examined to investigate the different grasping/sliding responses during tool-tissue interactions.

II. METHOD

A mechanical model was developed to simulate the interactions of the spleen tissue with a three-jaw large organ grasper (Fig 1). The spleen tissue was modeled as a deformable object with nonlinear viscoelastic properties. The jaws of the grasper were modeled as rigid links that always move in parallel, considering the parallelogram mechanism implemented in the grasper. The 3D geometry of the spleen was reconstructed in SolidWorks, based on the CT-scan images of a human subject, and then meshed into polyhedrons in Netgen. The vertexes and edges of the polyhedrons were considered as the mass points and the interconnected springs of the mass-spring-damper (MSD) model of the tissue, respectively (Fig 1).

A collision detection algorithm was designed and implemented to find the points at which the jaws contact with the tissue. The relative configuration of the three jaws of the grasper was described using a hollow cylinder, in which the

diameter decreased when the jaws were closed. Thus the jaws and tissue would contact only if a node of the tissue crossed through the cylinder surface. An algorithm was developed to detect the collision occurrence based on this simple concept. The Cartesian coordinates of the nodes on the tissue were converted into cylindrical coordinates and transferred so that the axis of cylindrical coordinate system coincides with the grasper axis. Then, the distances of the nodes from the axis were determined. This allowed the nodes that could potentially contact with the jaws to be identified. In the next stage, the nodes that their coordinates were consistent with those of the jaws were selected as the contact nodes.

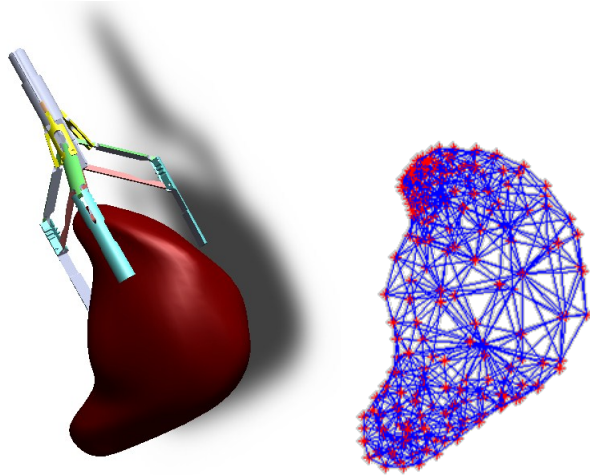


Fig 1. The components of the model including a three-jaw large organ grasper and a spleen tissue (left) and the mass-spring-damper model of the spleen tissue (right).

In a MSD model, the updating positions of the nodes are calculated through a differential equation system, in attendance of either force or geometrical boundary condition, so that all nodes always remain in force equilibrium. In our study, the boundary conditions of the MSD model of the tissue were specified considering the possible interactions of the contact nodes with the jaws. In a general view, the contact nodes are limited to move only in the plane of their corresponding jaws. For the slippage to happen, the external pull force should be larger than the tangential component of the contact force between the jaw and tissue. On the other hand, free-slippage grasping occurs if the tangential forces are smaller than the external pull.

Two types of boundary conditions were considered for the model to represent the slippage-free and slippage-accompanied grasping conditions. A geometrical boundary condition was associated with the slippage-free grasping, and a force boundary condition with the slippage-accompanied grasping (Fig 2). For the first case, the contact nodes were assumed to be completely stuck to their corresponding jaw. Thus, their kinematics, e.g. displacement, velocity and acceleration were the same as those of the jaw. For the latter case, a force constraint, representing the friction force, was applied to the contact nodes.

For formulation of the MSD model, the dynamic force equilibrium of each individual mass node was considered.

The discrete mass nodes, distributed throughout the model, and interconnected via a network of springs and dampers. For each mass node:

$$m_i \ddot{r}_i = F_i^{spring} + F_i^{nodal\ damping} + F_i^{external} \quad (1)$$

where F_i^{spring} and $F_i^{nodal\ damper}$ represent the total elastic and damping forces applied to node i from adjacent nodes, respectively, and $F_i^{external}$ is the external force applied to node i . Also, \ddot{r}_i is the acceleration vector for mass m_i : This equation might be extended to:

$$m_i \ddot{r}_i = \sum k_{ij} \Delta l_{ij} \frac{r_j - r_i}{\|r_j - r_i\|} - b_i \cdot \dot{r}_i + F_i^{external} \quad (2)$$

where:

$$\Delta l_{ij} = (r_j - r_i) - (r_{oj} - r_{oi}) \quad (3)$$

In above equations, r_i and r_j are the current and r_{oi} and r_{oj} are the initial position vectors for nodes i and a typical adjacent node j , respectively. Also, \dot{r}_i represents the current velocity vector for node i . The k_{ij} and b_i parameters stand for the spring constant which connect the mass point i to j and the nodal damping of node i .

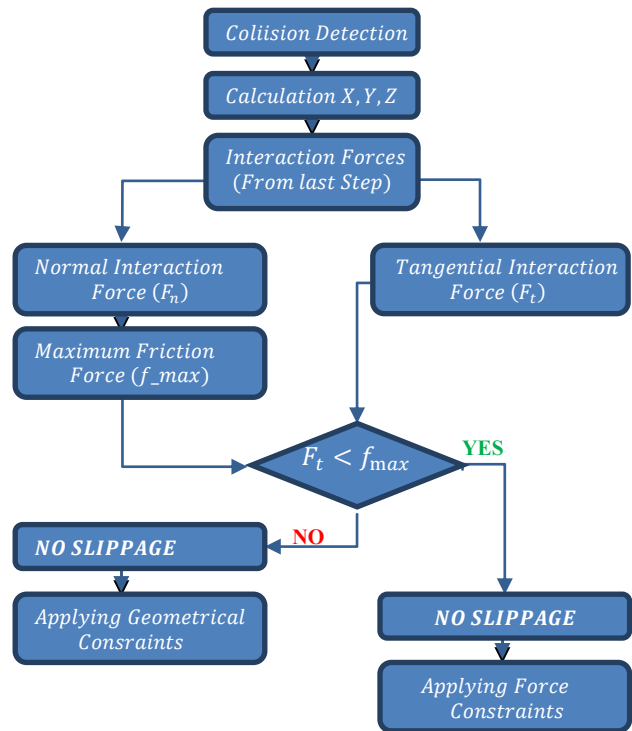


Fig. 2. The flowchart to determine the appropriate boundary conditions for contact nodes.

Updating of displacements requires simultaneous integration of the 2nd-order ordinary differential equations system (2). In numerical analysis, several implicit and explicit numerical integrating approaches, e.g. Euler's, Runge-Kutta and Finite Difference Methods, have been proposed to approach an approximate solution for ordinary differential equations. In this study, we used the Finite

Difference Method due to its high computational speed and acceptable accuracy.

In the next stage, parameter tuning was performed to obtain the relationship between the parameters of the MSD model and the mechanical properties of the tissue. In order to determine the parameters of the model, e.g., m , K_1 , K_2 , b_0 , b_1 , we followed an optimization procedure, in which the objective function was defined as the sum of the squared difference of the experimental data and the corresponding simulated response:

$$Error = \sum (F_i^{Experiment} - F_i^{Simulation})^2 \quad (4)$$

The Fmincon solver of MATLAB Optimization Toolbox (MATLAB, Mathworks Inc., Natick, Massachusetts) was used to minimize the objective function.

III. RESULT

The predictions of the model for deformation of the spleen tissue after grasping with the instrument are shown in figure 3. It was assumed that the grasper is being closed for 4 seconds, then its configuration is maintained for 7 seconds, and finally it starts to pull the tissue. The coefficient of friction between the jaws and tissue was assumed to be 0.6. Results indicate that the model was able to calculate deformation of the spleen, including its viscoelastic behavior reasonably, with an update rating of 150 Hz and rendering rating of 25 Hz on a conventional PC. The performance of the graphical rendering was also acceptable.

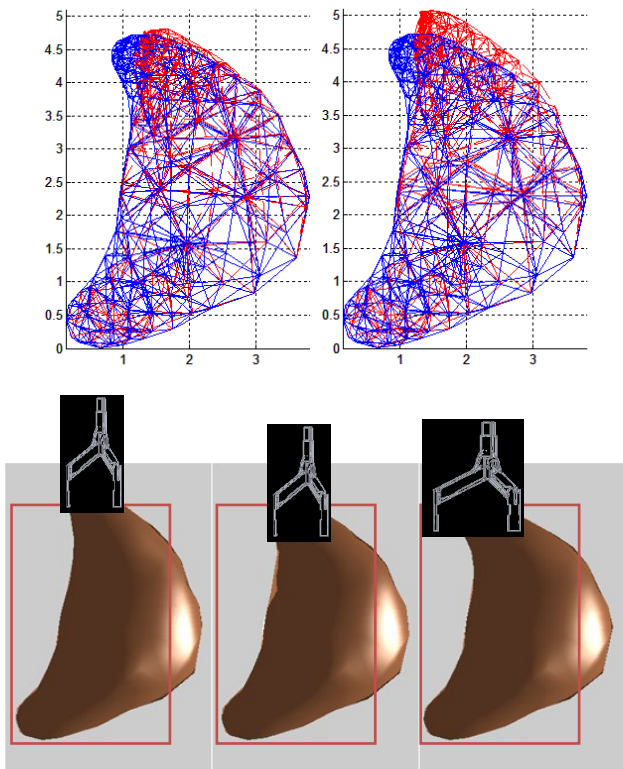


Fig. 3. The deformation of spleen tissue predicted by the model after initial grasping (top left) and after imposing pull force (top right). The results of graphical rendering are shown in the bottom.

The tool-tissue interaction forces, produced between the spleen tissue and the jaws of the grasper, are illustrated in figure 4, for original grasping condition and a case with a longer period of the jaws closing (5 seconds). The normal component of the force interaction shows a nearly linear increase when the jaws are closing, and then a sharp decrease due to stress relaxation, when they are stopped. After applying the pull force, a slight decrease is also observed in the normal interaction force. For the tangential force component, the model predicted a nonlinear increase which was then followed by a decreasing pattern when the sliding started.

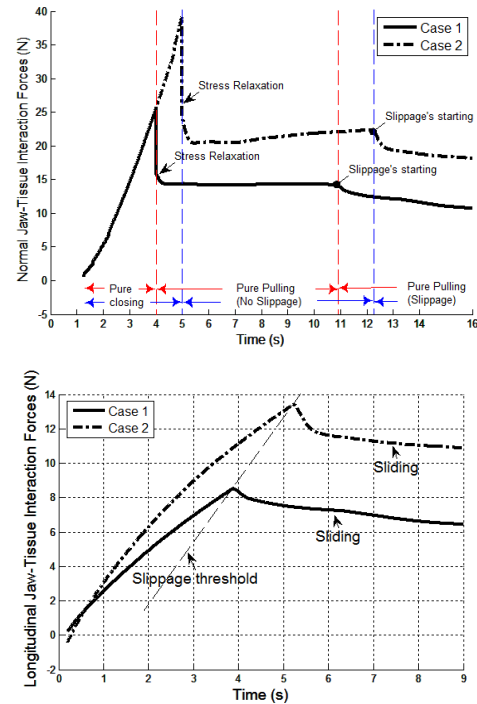


Fig. 4. The normal (top) and tangential (bottom) force components of the tool-tissue interaction ($\mu=0.6$)

The effect of the friction coefficient on the normal and tangential force components of the tool-tissue interaction are illustrated in figure 5. Higher friction did not affect the normal component of the grasping force. However, it caused the decrease of the normal force, due to sliding, to start at a later period. The effect of the friction coefficient on the tangential force component was quite considerable. With higher frictions, the tangential force increased largely and the slippage occurred at much higher pulling forces.

IV. DISCUSSION

Several different approaches have been proposed for modeling of deformable objects in real-time surgery simulation. Physically based approaches [16], include a wide range of methods from continuum based methods, e.g., finite element, to discrete methods, e.g., mass-spring and meshless models. Although the continuum based methods are considered to provide a more accurate physical simulation of

the tissue's behavior, they are difficult to be implemented in real time, due to their high computational cost [17]. This would be more problematic if the nonlinear and viscoelastic behavior of the tissue are to be considered. On the other hand, the discrete models, such as mass-spring-damper, are based on a local description of the material and allow for large deformations and displacements to be simulated in real time [18]. In spite of their lower accuracy, they are simple for implementation and have a low computational cost which makes them an appropriate solution for surgical simulation applications in which a qualitative agreement with reality is often adequate.

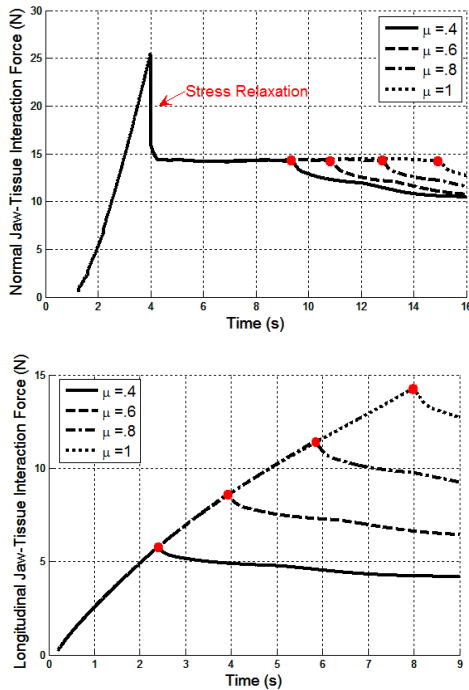


Fig. 5. The normal (top) and tangential (bottom) force components of the tool-tissue interaction for $\mu=0.6$, $\mu=0.6$, $\mu=0.8$, $\mu=1$ (Red points represent the start of slippage).

The mass-spring-damper model of our study was capable of simulation of the complicated mechanical behavior of nonlinear viscoelastic spleen tissue, and its interactions with a surgical grasper in real time. We were unable to verify our results in view of the fact that no comparable experimental data were found in the literature. However, our results seem qualitatively acceptable and could mimic the general aspects of the tissue mechanical behavior and the tool-tissue force interactions. The stress relaxation of the tissue, when the jaws closing is stopped (Fig 4), is a representative of the models capability to simulate the viscoelastic behavior of the spleen tissue. On the other hand, the tool-tissue interactions, including the slippage-free grasping and slippage-accompanied grasping were well simulated by the model (Fig 4). Also, the effects of the coefficient of friction (Fig 5) predicted by the model is reasonable. Considering the fact that surgical simulation systems do not require very accurate and realistic response, the proposed method is thought to fulfill the basic requirements of such systems.

REFERENCES

- [1] Mack, M.J., Minimally invasive and robotic surgery. *Journal of the American Medical Association*, 2001; **285**(5), pp. 568-572.
- [2] Schwenk, W., B. Böhm, and J.M. Müller, Postoperative pain and fatigue after laparoscopic or conventional colorectal resections: A prospective randomized trial. *Surgical Endoscopy*, 1998; **12**(9), pp. 1131-1136.
- [3] Kühnapfel, U., H.K. Çakmak, and H. Maaß, Endoscopic surgery training using virtual reality and deformable tissue simulation. *Computers & Graphics*, 2000; **24**(5), pp. 671-682.
- [4] De, S., J. Kimb, Y.J. Lima, and M.A. Srinivasan, The point collocation-based method of finite spheres (PCMFS) for real time surgery simulation. *Computers & Structures*, 2005; **83**(17-18), pp. 1515-1525.
- [5] Basdogan, C., C.H. Ho, and M.A. Srinivasan, Virtual environments for medical training: graphical and haptic simulation of laparoscopic common bile duct exploration. *IEEE/ASME Transactions on Mechatronics*, 2001; **6**(3), pp. 269-285.
- [6] Sierra, R., M. Bajka, and G. Székely, Tumor growth models to generate pathologies for surgical training simulators. *Medical Image Analysis*, 2006; **10**(3), pp. 305-316.
- [7] De, S., et al., Multimodal simulation of laparoscopic Heller myotomy using a meshless technique. *Stud Health Technol Inform*, 2002; **85**, pp. 127-32.
- [8] Laycock, S.D. and A.M. Day, Incorporating haptic feedback for the simulation of a deformable tool in a rigid scene. *Computers & Graphics*, 2005; **29**(3), pp. 341-351.
- [9] Srinivasan, M.A. and C. Basdogan, Haptics in virtual environments: Taxonomy, research status, and challenges. *Computers and Graphics*, 1997; **21**(4), pp. 393-404.
- [10] Wu, X., et al., Adaptive nonlinear finite elements for deformable body simulation using dynamic progressive meshes. *Computer Graphics Forum*, 2001; **20**(3), pp. 349-358.
- [11] Zhong, H. and T. Peters, A real time hyperelastic tissue model. *Computer methods in biomechanics and biomedical engineering*, 2007; **10**(3), pp. 185-193.
- [12] Basafa, E. and F. Farahmand, Real-time simulation of the nonlinear visco-elastic deformations of soft tissues. *International Journal of Computer Assisted Radiology and Surgery*, 2011; **6**, pp. 297-307.
- [13] Yi-Je, L., et al. Soft Tissue Deformation and Cutting Simulation for the Multimodal Surgery Training. in *Computer-Based Medical Systems*, 2006. CBMS 2006. 19th IEEE International Symposium on. 2006.
- [14] Paloc, C., A. Faraci, and F. Bello, Online remeshing for soft tissue simulation in surgical training. *IEEE Comput Graph Appl*, 2006; **26**(6), pp. 24-34.
- [15] Doblaré, M., et al., On the employ of meshless methods in biomechanics. *Computer Methods in Applied Mechanics and Engineering*, 2005; **194**(6-8), pp. 801-821.
- [16] Nealen, A., et al., Physically based deformable models in computer graphics. *Computer Graphics Forum*, 2006; **25**(4), pp. 809-836.
- [17] Tang, Y.M., A.F. Zhou, and K.C. Hui, Comparison of FEM and BEM for interactive object simulation. *Computer Aided Design*, 2006; **38**(8), pp. 874-886.
- [18] Debunne, G., et al. Dynamic real-time deformations using space & time adaptive sampling. in *Proceedings of the ACM SIGGRAPH Conference on Computer Graphics*, 2001; Los Angeles, CA.